EFFECTS OF SCALE IN PREDICTING GLOBAL STRUCTURAL RESPONSE[1]

R. B. Deo
H. P. Kan

Northrop Corporation
Aircraft Division
Department 3853/82
One Northrop Avenue
Hawthorne, California

ABSTRACT

In the course of previous composite structures test programs, the need for and the feasibility of developing analyses for scale-up effects has been demonstrated. The analysis techniques for scale-up effects fall into two categories. The first category pertains to developing analysis methods independently for single, unique failure modes in composites, and using this compendium of analysis methods together with a global structural model to identify and predict the response and failure mode of full-scale built-up structures. The second category of scale-up effects pertains to similitude in structural validation testing. In this latter category, dimensional analysis is used to develop scale-up laws that enable extrapolation of sub-scale component test data to full-scale structures. This Work-In-Progress paper describes the approach taken and some accomplishments in the first category of analysis for scale-up effects. A building block approach is proposed where each structural detail is analyzed independently; then, the probable failure sequence of a selected component is predicted, taking into account load redistribution subsequent to first element failure. Layup dependence of composite material properties severely limits the use of the dimensional analysis approach and these limitations are illustrated by examples.

INTRODUCTION

The high cost of design and testing of full-scale composite structures has necessitated the use of scale model testing and analytical scaling techniques for structural response prediction. Recent experience (References 1 and 2) in structural testing indicates that scale-up effects in composite structures are strongly influenced by the structural configuration and substructural arrangement. This is because of the multitude of failure modes that may occur in built-up composite structure. Even in the case of structural elements with a single unique failure mode, scaling effects are influenced by factors unique to composite materials, such as layup, (References 3 through 7) and, therefore, a complete set of scaling rules can not always be established.

[1] This work was performed under NASA/Northrop Contract NAS1-18842, entitled "Innovative Composite Fuselage Structures."

The analysis techniques for scale-up effects fall into two categories. The first category pertains to developing analysis methods independently for single, unique failure modes in composites and using this compendium of analysis methods together with a global structural model to identify and predict the response and failure mode of full-scale, built-up structures. Examples of this technique are the building-block approach of Reference 1, the semi-empirical approach of Reference 2, and the global/local analysis procedure of Reference 8. The second category of scale-up effects pertains to similitude in structural validation testing. In this category, dimensional analysis is used to develop scale-up laws that enable extrapolation of sub-scale component test data to full-scale structures. The applicability of this technique is limited to self-similar scale models. Examples in this category are the static and dynamic beam and plate models of References 3 through 7.

In this Work-In-Progress paper, both approaches to scale up law development are reviewed. The applicability and limitations of the existing methods are summarized. Layup dependence of composite material properties severely limits the use of the dimensional analysis approach and these limitations are illustrated by examples. A simplified similitude relationship for shells and curved panels is presented. Finally, the building-block approach, where each structural detail is analyzed independently, and the probable failure sequence on a selected component is predicted, taking into account load redistribution subsequent to first element failure is described.

BACKGROUND

Several scale-up law development approaches have been investigated in the literature. Application of the principles of similitude to transversely impacted composite beams was studied in Reference 3. In this reference, a set of scaling rules was established for the dynamic response of composite beams subjected to low velocity impact. Potential scaling conflicts were also discussed. A test program was then conducted to verify the rules established from dimensional analysis. The results of the tests indicated that within elastic range of beam response, the duration of impact and the impact force closely followed the theoretical scaling rules. The impact duration scaled as the geometric scale factor and the impact force as the scale factor squared. The scatter in the test data was approximately ±10 percent, which was attributed to the deviation of the specimen thickness from the nominal thickness of the laminate.

Two important observations were made in Reference 3. First, the rate effects were found to be insignificant for the material and layup considered. Since the rate effect may cause a scaling conflict in the dimensional analysis, this observation justifies the use of the principle of similitude for certain type of composites. Secondly, where the impact resistance strength is concerned, significant size effects were noted. Smaller specimens were stronger than the larger specimens. The latter observation, if verified in general, will limit the scale-up of model tests.

Experimental investigations of scaling rules for composite plate response to impact were conducted in References 4 and 5. In these references, a set of scaling rules was established based on dimensional analysis. By considering the equations of motion of the plate, and assuming that material properties were unchanged, References 4 and 5 showed that geometric dimensions must be scaled uniformly. That is, the scale factors for length, width, and thickness of the plate should be identical. The

time parameter must also be scaled in accordance with the geometric scale factor. The experimental results in these references showed that, when the impact velocity is sufficiently low so that no significant material damage is produced, the strain response closely followed the scaling rules. The strain response was the same for different size specimens with time scaled by the geometric factor and the impactor mass scaled by the cube of the geometric factor.

It should be noted that in the preceding studies (References 3, 4, and 5) damage due to impact was not considered in scaling. No attempts were made to relate the extent of damage with specimen size. This is because the extent of impact damage is known to be a strong function of size and boundary conditions and is usually analyzed by applying fracture mechanics. This requires more complex scaling analysis.

Scaling effects in the large deflection response of composite beams were studied in References 6 and 7. Reference 6 investigated the static response and Reference 7 investigated the dynamic response. The beams were loaded under an eccentric axial compressive load to promote large deflections and global failure. The static test results (Reference 6) showed that the beam response followed the scaling rules in the small deflection, elastic region; however, deviations from the scaling rules appeared as the beams underwent large deflections and rotations. That resulted in a significant size effect in the failure behavior. The smaller beams failed at a higher normalized load and higher normalized end displacement than the larger beams. This observation of size effects agrees with the results of Reference 3.

Impact tests were conducted in Reference 7 on the large deflection beam used in Reference 6. Scaling rules, based on dimensional analysis, were also established in Reference 7. These rules are similar to those proposed in References 3 through 5. The experimental results in Reference 7 indicated that load and strain responses of the unidirectional beam followed the scaling rules quite well. However, the results were inconsistent for specimens with other laminate layups (cross-ply, angle-ply, and quasi-isotropic). The significant size effects on failure behavior observed in static tests (Reference 6) were not found in the impact test results of Reference 7.

From the results of References 3 through 8, the following general observations can be made on scaling of composites.

1. Scaling rules based on dimensional analysis are not unique. Different sets of scaling rules may be established for one type of structure.

2. Simple scaling rules can only be established for the same family of laminate layups. This significantly limits the general application of the principle of similitude on actual structures.

3. Size effects exist in composite structures, which may be caused by material inhomogeneity. Direct application of the scaling rules may result in unconservative estimates of full-scale structural response.

4. Structural response beyond the elastic limit does not follow simple scaling rules. Therefore, the principle of similitude may not be useful for failure prediction.

5. Extensive tests are required to verify the applicable scaling rules and establish guidelines for test data interpretation.

PRACTICAL APPLICATION EXAMPLES

The applicability of classical dimensional analysis principles in composite structural mechanics was assessed by examining two fundamental problems: (1) axial tension loading of a narrow laminate and (2) buckling of a narrow laminated plate. These problems were selected to highlight two important parameters in the scaling of composites - layup and stacking sequence. These parameters are not relevant to the scaling of metallic structures but have significant effects in scaling of composites. The applicability of classical dimensional analysis is illustrated by the following examples.

Consider a 24-ply baseline laminate of 1-inch width and subjected to tensile loading along the 0 degree direction. The laminate stacking sequence is $[\pm 45/0_2/\pm 45/0_2/\pm 45/90/0]_s$, which gives a (42/50/8) distribution of plies. The lamina mechanical properties are

$E_L = 18.7 \times 10^6$ psi $\qquad \nu_{LT} = 0.3$

$E_T = 1.9 \times 10^6$ psi $\qquad t = 0.0052$ in.

$G_{LT} = 0.85 \times 10^6$ psi $\qquad \epsilon_f = 0.011$ in/in.

The calculated Young's modulus in the loading direction is $E_x = 9.977 \times 10^6$ psi. The strain response of the laminate can be approximated by

$$\epsilon = \frac{P}{AE_x} = \frac{P}{nbtE_x}, \tag{1}$$

where, P is the applied load, n is the number of plies, and b is the laminate width. To scale down the laminate and simulate the strain response, two assumptions were made. First, it was assumed that symmetry of the laminate is maintained and second, that the orthotropy of the laminate is maintained throughout the scaling process. These assumptions ensure that Equation 1 holds true for all of the scaled-down laminates.

Now consider the failure load P_f based upon the maximum strain criterion. Equation 1 becomes

$$P_f = nbtE_x\epsilon_f \tag{2}$$

The failure load calculated for the baseline laminate is 13,681 lb. For cases of constant modulus E_x, such as metals, the failure load would vary linearly with the cross-sectional area of the specimen. This is shown by the solid line in **Figure 1**. For composite laminates, however, the modulus E_x is a function of the thickness (number of plies) and the layup. Scaling in thickness by adding or reducing the number of plies gives rise to a nonlinear relationship between the failure load and cross-sectional area. To illustrate this point, suppose that the laminate width is given a constant value of b = 1.0 inch while the number of plies is reduced. The failure loads will depend upon the type of plies (0°, ±45°, 90°) removed from the laminate. For example, if the baseline 24-ply laminate is reduced to 22 plies by removing two 0 degree plies, two ±45 degree plies, or two 90 degree plies, the corresponding failure loads are 11,500 lb, 13,300 lb, and 12,900 lb, respectively. As the

number of plies is reduced still further, the possible failure loads are found to lie in an envelope centered about the linear failure load versus cross-sectional area relationship as shown in **Figure 1**.

To further illustrate the issues pertinent to the scaling of composite structures, consider a second problem involving a narrow laminated composite plate subjected to axial compressive load. The buckling load for a plate of this kind with clamped ends and free edges is

$$N_{cr} = k \left(\frac{2\pi}{L}\right)^2 D_{11} \qquad (3)$$

where

L = total length of the plate

D_{11} = bending rigidity in the loading direction

k = a constant equal to 1.0306 for the first buckling mode

From Equation 3, the scaling parameters to be considered in this problem are L and D_{11}. Because D_{11} depends upon the thickness, modulus, and stacking sequence, this problem represents one higher level of complexity than the problem discussed previously.

Consider the same 24-ply baseline laminate as in the first problem, with an unsupported length L = 3.0 inches. The axial bending rigidity of the plate is 1,777 lb-in. If the modulus is constant, as for metals, D_{11} varies with h^3 (h is the total thickness). As the thickness reduces to 22 plies, the possible combinations of layup and stacking sequence along with the associated bending rigidity and buckling load are given in **Figure 2**. **Figure 3** shows the buckling load as a function of laminate thickness. The buckling loads for the composite laminate fall in an envelope centered about the solid curve, which is the buckling load versus thickness relationship for a constant modulus material.

The results shown in **Figures 1 and 3** show that scaling in composites, even for the simplest structural mechanics problems, involves more than dimensional parameters. Because of the multiplicity of possible laminate constructions, structural mechanics methods of analysis must be used to develop similitude rules.

Similar results can be obtained for two-dimensional problems. The thickness, ply-orientations and stacking sequence effects on bending of a rectangular composite plate subjected to uniform lateral pressure is shown in **Figure 4**. The buckling load of a simply supported rectangular plate is shown in **Figure 5**. Both **Figures 4 and 5** show that structural response deviates from the classical dimensional analysis results. The deviation is caused by the layup and stacking sequence effects on the plate rigidity parameters, D_{ij}. In comparing the results of the two-dimensional problems with that of one-dimensional, **Figures 4 and 5** show a narrower band in the structural response. This occurs because the results of the one-dimensional problems are affected only by the axial properties E_x and D_{11}, whereas, the results of the two-dimensional problems are affected by all components of the in-plane mechanical properties. The overall effect of all four rigidity components (D_{11}, D_{12}, D_{22}, D_{26}) is less significant than that of a single component.

SPECIALIZED SCALING TECHNIQUES IN COMPOSITES

The previous section discussed the difficulties in direct application of the principle of similitude in composites. It was also pointed out that scale model can be designed with the aid of structural mechanics. In this section, an analytical procedure to design scale models is presented. The procedure is similar to the one proposed in Reference 8 and is illustrated by the following example.

Consider an unstiffened composite cylinder of radius R_s, thickness t_s, and length L_s. The scaling parameters significant to buckling can be divided into three categories:

1. Load Parameter

$$P_r = (N_{cr})_m/(N_{cr})_s \tag{4}$$

where N_{cr} is the buckling load per unit length around the cylinder circumference.

Subscripts m and s denote the scaled model and the full-scale structure, respectively.

2. Geometric Parameters

Length Ratio	$L_r = L_m/L_s$	(5)
Radius Ratio	$R_r = R_m/R_s$	(6)
Thickness Ratio	$t_r = t_m/t_s$	(7)

3. Property Parameters

Modulus Ratio	$E_r = E_m/E_s$	(8)
Stiffness Ratio	$D_r = D_m/D_s$	(9)

where E and D are Young's modulus and bending rigidity, respectively.

The load parameter P_r is a predetermined design factor for the model. The load requirement for the test model is usually higher than the actual structure. In the case where the exact buckling load of the structure is to be simulated, $P_r = 1.0$.

The geometric and property parameters interact when buckling is considered. For composite structures, the property parameters are usually not unique because of the anisotropy of the materials. These parameters are also affected by the thickness parameter because of the ply orientations. Therefore, it is not possible to establish a simple scaling law for composite structures as discussed in the preceding section.

In the present analysis, the scaled model is designed using an iterative procedure. The analysis method for symmetric buckling of isotropic cylinders is first used to estimate the key scaling parameters. The buckling load of an isotropic cylinder with R >> t is given in Reference 9 as

$$N_{cr} = \frac{2}{R}(EDt)^{1/2} \tag{10}$$

Based on this expression, the key scaling parameters can be written as

$$R_r = \frac{1}{P_r}(E_r D_r t_r)^{1/2} \tag{11}$$

$$t_r = \frac{(R_r P_r)^2}{E_r D_r} \tag{12}$$

$$E_r = \frac{(R_r P_r)^2}{t_r D_r} \tag{13}$$

$$D_r = \frac{(R_r P_r)^2}{E_r t_r} \tag{14}$$

For isotropic material

$$D = \frac{Et^3}{12(1-\nu^2)} \tag{15}$$

Assuming that the test model is fabricated from the same material as the full-scale structure, then the Poisson ratios $\nu_m = \nu_s$ and the stiffness ratio becomes

$$D_r = E_r t_r^3 \tag{16}$$

Equation 10 indicates that the length parameter is an arbitrary number if only buckling load is to be simulated. The length of the cylinder controls the buckling mode, but not the buckling load.

For composite cylinders, the scale parameters are first estimated using Equations 11 through 16. Then the following procedure is used:

1. Define the load requirement (P_r).

2. Select the radius and length ratio (R_r, L_r). Because length has no significant effect on buckling load, assume $L_r = R_r$.

3. Maintain approximately the same axial Young's modulus ($E_r \approx 1.0$).

4. Estimate t_r from Equations 12 and 16:

$$t_r^2 = P_r R_r \tag{17}$$

5. Based on the estimated t_r, determine the practical thickness of the model, t_m. The practical thickness is determined based on the number of plies.

6. Determine the ply orientations. The ply orientations should be similar to the full-scale structure in the initial estimate, because $E_r \approx 1.0$.

7. Determine the laminate stacking sequence based on D_r given in Equation 14. The practical rules for laminate stacking should be taken into consideration.

8. Conduct orthotropic (anisotropic) buckling analysis to confirm P_r.

9. Perform iterations until the required P_r is obtained.

The following example problem illustrates this procedure:

Consider a full-scale cylinder 45 inches in radius and 25 inches in length. The cylinder is made of AS4/3501-6, 16-ply $(\pm 45/0_2/\pm 45/90/0)_s$ laminate with a thickness of 0.0832 inch. A 1/5 subscale model with a load requirement of $P_r = 1.5$ will be designed.

For the full-scale cylinder buckling,

$$(N_{cr})_s = 669.66 \text{ lb/in}$$

The required buckling load for the subscale model is

$$(N_{cr})_m = 1005 \text{ lb/in}$$

The dimension requirement gives

$$R_m = 9.0 \text{ in}$$

$$L_m = 5.0 \text{ in}$$

From Equation 17 the initial estimate of the model thickness is

$$t_r = (P_r R_r)^{1/2} = 0.548$$

or

$$t_m = (0.548)(0.0832) = 0.0456 \text{ in}$$

For the material considered, a 9-ply laminate is required, which has the nominal thickness of 0.0468 inch.

For $E_r \approx 1.0$, the percentage distribution of 0°, 45°, and 90° plies for the 9-ply laminate is either (33.3/55.6.11.1) or (44.4/44.5/11.1). A $(\pm 45/0_2/90/0_2/\mp 45)_T$ was chosen in this example. A 9-inch radius cylinder with this laminate resulted in

a buckling load of 939.6 lb/in or $P_r = 1.4$ which is below the load requirement of 1.5. Hence, further iteration on the scale parameters is required. Two approaches to vary the subscale model were considered in order to meet the load requirement. First, if the dimensional requirement ($R_r = 0.2$) can be changed, then the load requirement can be met by reducing the radius to 8.4 inches. With this radius, the buckling load increases to 1011 lb/in or $P_r = 1.510 > 1.50$. Second, by changing the laminate stacking sequence to $(45/0/-45/0/90/0\text{-}45/0/45)_T$ with all other parameters fixed, the buckling load increases to 1051 lb/in or $P_r = 1.569$.

The final values for the subscale model (for illustration purposes only) are

$R_m = 8.4$ in

$L_m = 4.7$ in

$t_m = 0.0468$ in 9-ply $(\pm 45/0_2/90/0_2/\mp 45)_T$

The scaling parameters are

D_r	= 0.15	(0.164)
E_r	= 1.11	(1.0)
t_r	= 0.5625	(0.548)
P_r	= 1.505	(1.50)
R_r	= 0.187	(0.2)
L_r	= 0.188	(0.2)

Numbers in parentheses denote initial estimates.

To further scale down the structure, a cylindrical panel instead of a subscale cylinder can be considered. This requires determining the panel width (or central angle θ), with all other parameters unchanged. Parametric study indicates that for simply supported cylindrical panels, the panel buckling load (N^P_{cr}) is higher than that of a complete cylinder (N^C_{cr}). However, the panel buckling load approaches the buckling load of a complete cylinder as the panel width increases. Beyond a minimum panel width, N^P_{cr} is within 5 percent of N^C_{cr} as shown in **Figure 6**. The minimum width depends on the radius of the cylinder and can be determined analytically. For the example cylinder discussed earlier, the minimum panel width is 4.75 inches (or central angle $\theta = 32.4°$).

Figure 6 shows the effect of panel width on buckling load. From this figure, it can be seen that the buckling load of the full-scale cylinder can be experimentally determined by testing a curved panel with a minimum width of 4.75 inches. It may be noted, that although the buckling load of a complete cylinder can be simulated by a portion of a subscale cylinder (panel), the buckling mode is difficult to simulate.

THE BUILDING BLOCK APPROACH

As discussed earlier, another category of scale-up laws pertains to using structural analysis methods with a structural model to identify and predict the response and failure mode of full-scale built-up structures. These scale-up effects are investigated through a building block approach. In the following paragraphs, this approach is first illustrated by an example. The analytical development procedure is then discussed.

An example illustrating this category of scale-up laws is that of post-impact compression strength of coupons and built-up 3-spar panels representative of an upper wing skin. Scale-up effects test data and the accompanying analysis for this case were developed in Reference 2. The scale-up effects observed from test data in this example are shown in **Figure 7**. This figure compares the post-impact compression strength of the 5-inch wide coupon to that of built-up panels of similar layup and thickness subjected to the same level of impact energy. The shift in strength data from coupons to 3-spar panels is indicative of the scale-up effect.

The accompanying structural mechanics scale-up analysis in Reference 2 was based on an extensive set of data for static strength of impact-damaged built-up composites. It was observed, in the reference, that failure of damaged coupons was single-stage, with damage propagating from the impact site to the edges at the failure load. For a built-up structure, the overall post-impact strength was significantly influenced by the structural configuration. It was observed that failure in most of the 3-spar panels was in two stages. At initial failure, the damage propagated to the spar fastener lines. The initial failure load (strain) corresponded to the final failure load of coupon specimens. The damage propagation was arrested by the spars, with final failure taking place at a higher applied load.

A semi-empirical analysis method was developed in Reference 2 to predict the scale-up effects on post-impact damage strength. The model for the coupon failure is based on an elastic stiffness reduction technique. The structural configuration scale-up effects on residual strength are incorporated in the stiffness reduction to predict the two-stage failure.

A comparison of observed and predicted post-impact failure strains is shown in **Figure 8**. The figure shows that the predicted initial and final failure strains agree well with test data. This structural mechanics scale-up law to predict residual compression strength after impact was exercised on a large test data base for built-up structures, including a full-scale wing box. **Figure 9** shows the test analysis correlation for a wide range of structural geometries and materials.

The above example illustrates the feasibility of and the methodology for the development of structural mechanics scale-up laws for composite structures.

The building block approach used here is similar to the experimental approach proposed in Reference 1 and summarized in **Figure 10**. This figure shows that design development testing is characterized by five levels of complexity, with the fifth level assigned to the full-scale component.

The wing skin coupon specimens represent the first complexity level in the building-block approach and simulate simple tension and compression failure modes. Six specimen types were tested in Reference 1. These were either open or filled hole

specimens tested under tension (lower wing skin) or compression (upper wing skin) with laminates representing different locations on an actual fighter wing structure. At this level of complexity, the analysis task is to correctly predict the failure stress/strain and failure load from the available lamina properties. The required analytical tools are open and filled hole analyses and an appropriate failure criterion. Scaling law development at this level of complexity involves correlating observed and predicted failure stress, strain, and loads. Analysis and correlation for the wing skin coupon specimens will be carried out during the next reporting period.

The second complexity level in the test program of Reference 1 contains three specimen types. Each of these specimens has two potential failure modes. An upper skin/rear spar mechanical joint (WE-2) was designed to check the influence of load transfer on compression strength. Potential failure modes for this specimen are laminate failure and bearing failure at a fastener hole. Loaded hole analysis will be conducted on this specimen. Both bearing and net-section failure criteria will be required for failure prediction. The scaling law development here will involve the use of open and filled hole test data to predict (or correlate) the specimen failure load and failure mode.

Another specimen type at the second level of complexity is an intermediate spar/lower skin cocured joint (WEC-1). This specimen is designed to check spar web strength in the presence of a fuel drain hole and the cocured bonded joint strength under combined shear, fuel pressure and chordwise loading. Potential failure modes are web failure at the fuel drain hole and bondline failure in the cocured joint. The applicability of the open hole analysis will be re-examined for this problem. In addition, stress analysis of the bondline will be conducted.

A third specimen, the front spar/skin joint (WE-1) shown in **Figure 10**, is representative of the graphite/epoxy front spar-to-skin joint. The specimen was subjected to corner bending and shear induced by fuel pressure. The potential failure modes for this specimen are joint failure (fastener pull-through and adhesive failure) and interlaminar tension failure at the corner. Joint analysis and corner radius analysis will be conducted and failure criteria will be established for this specimen type. Coupon test data are not applicable for this specimen type because the potential failure modes are both out-of-plane in nature.

The third complexity level in the test program of Reference 1 is represented by an intermediate spar/pylon rib load transfer joint (WEC3), and is designed to check load transfer from the discontinuous spar into the rib and back to the spar. This specimen combines the potential failure modes of the wing coupons and WEC-1, i.e., upper and lower skin failures at a rib attachment fastener hole, spar web failure and intermediate spar/lower skin failure in the cocured joint. The fourth and final level of complexity in the torsion box design development testing is represented by the wing subcomponent (WS-1) which is a three bay box beam, and root rib/aft trunnion subcomponent which represents the highly loaded root rib/aft trunnion area. All of the failure modes of the wing coupons, WE-2, WE-1, and WEC-3 are represented in the WS-1 specimen. In addition, an upper skin access hole provides a further potential failure mode. The fifth level of complexity is the wing component, which is fully representative of the actual wing structure.

Comprehensive structural analysis will be conducted at the subcomponent level and the component level for both the wing and fuselage structures. The analysis results will then be correlated with test data to establish scaling laws.

SUMMARY

Analytical techniques for scale-up effects have been reviewed. The advantages and limitations of applying the principles of similitude to composite structures have been summarized and illustrated by simple examples. An analytical procedure was formulated to design scale models of an axially compressed composite cylinder. A building-block approach was outlined where each structural detail is analyzed independently and the probable failure sequence of a selected component is predicted, taking into account load redistribution subsequent to first element failure. Details of this building-block approach are under development.

REFERENCES

1. Whitehead, R. S., et al., "Composite Wing/Fuselage Program," AFWAL-TR-88-3098, Volumes I-IV, February 1989.

2. Horton, R. E., Whitehead, R. S., et al., "Damage Tolerance of Composites," AFWAL-TR-87-3030, Volumes I, II, and III, July 1988.

3. Morton, J., "Scaling of Impact-Loaded Carbon-Fiber Composites," AIAA Journal, Volume 26, No. 8, August 1988, pp 989-994.

4. Dian, Y. and Swanson, S. R., "Experimental Measurement of Impact Response in Carbon/Epoxy Plates," proceedings of the 30th AIAA/ASME/ASCE/AHS/ASC Structures, Structural Dynamics, and Materials Conference, April 1989, pp 1023-1029.

5. Dian, Y, Swanson, S. R., Nuismer, R. J., and Bucinell, R. B., "An Experimental Study of Scaling Rules for Impact Damage in Fiber Composites," Journal of Composite Materials, Volume 24, May 1980, pp 559-570.

6. Jackson, K. E. and Fasanella, E. L., "Scaling Effects in the Statis Large Deflection Response of Graphite-Epoxy Composite Beams," proceedings of the American Helicopter Society National Technical Specialist's Meeting on Advanced Rotorcraft Structure, October 25-27, 1988.

7. Jackson, K. E. and Fasanella, E. L., "Scaling Effects in the Impact Response of Graphite-Epoxy Composite Beams," SAE General Aviation Aircraft Meeting and Exposition, Wichita, Kansas, April 11-13, 1989, Paper No. 891014.

8. McCullers, L. A. and Neberhans, J. D., "Automated Structural Design and Analysis of Advanced Composite Wing Models," Composite and Structures, Volume 13, 1973, pp 925-935.

9. Timoshenko, S. P. and Gere, J. M., Theory of Elastic Stability, McGraw Hill Book Company, New York, 1961.

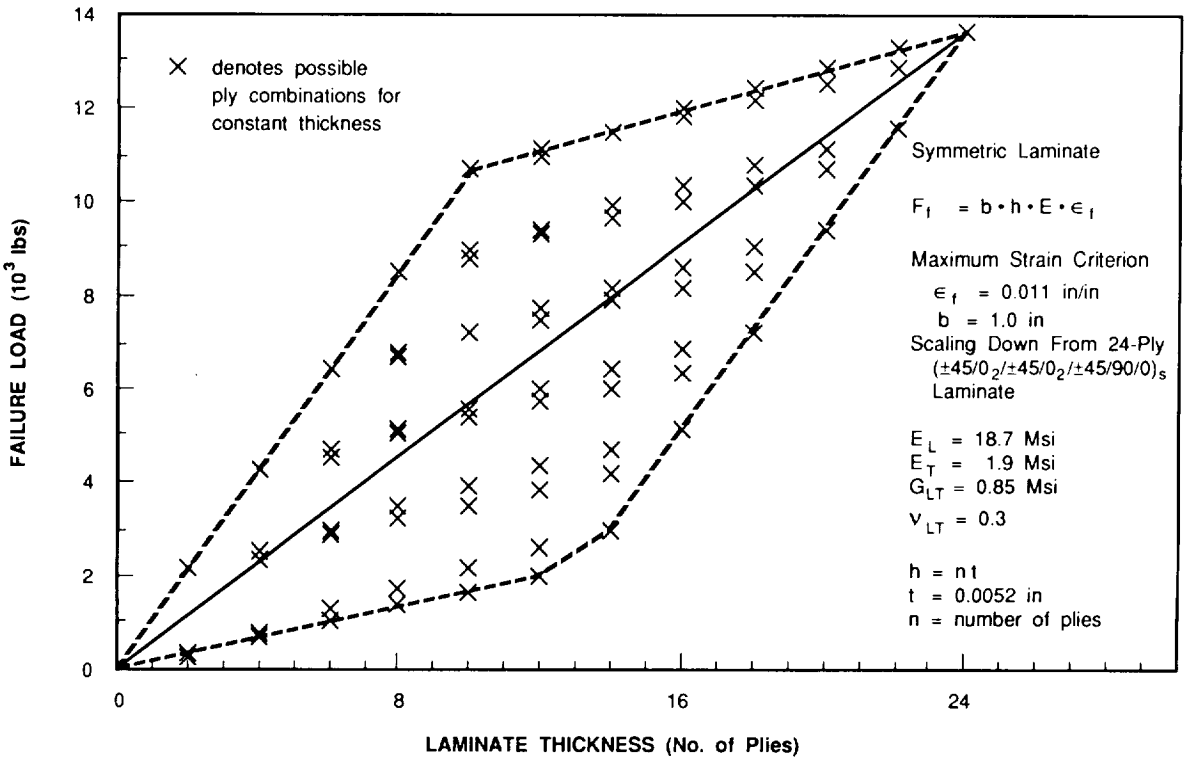

Figure 1. Tensile Failure Load of a Narrow Composite Plate as a Function of Laminate Thickness.

LAYUP	STACKING SEQUENCE	D_{11} (lb-in)	N_{cr} (lb-in)
(45.5/45.5/9)	$[45/0_2/\pm 45/0_2/\pm 45/90/0]_s$	1541	6966
	$[\pm 45/0_2/45/0_2/\pm 45/90/0]_s$	1421	6424
	$[\pm 45/0_2/\pm 45/0_2/45/90/0]_s$	1358	6137
(36/55/9)	$[\pm 45/0/\pm 45/0_2/\pm 45/90/0]_s$	1222	5526
	$[\pm 45/0_2/\pm 45/0/\pm 45/90/0]_s$	1314	5940
	$[\pm 45/0_2/\pm 45/0_2/\pm 45/90]_s$	1358	6143
(45/55/0)	$[\pm 45/0_2/\pm 45/0_2/\pm 45/0]_s$	1360	6150

Figure 2. Possible 22-Ply Laminates in Example Buckling Problem.

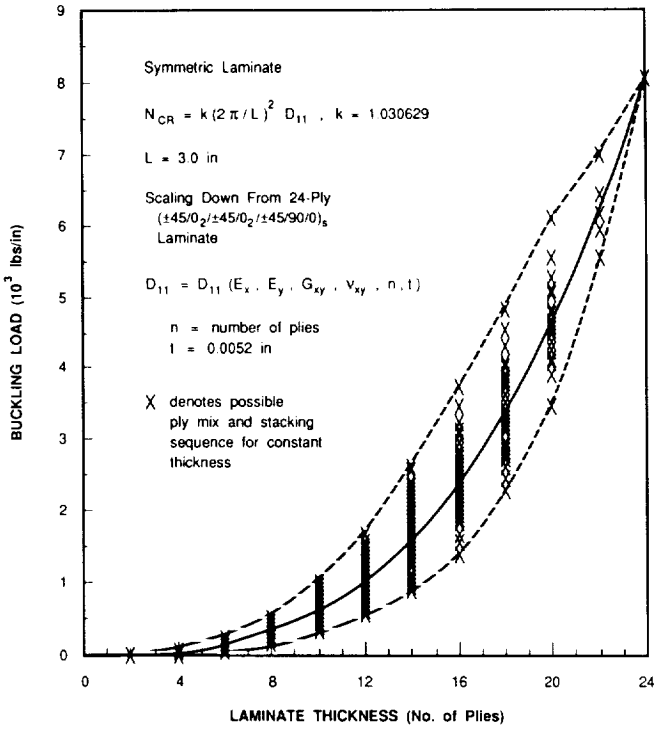

Figure 3. Buckling Load as a Function of Laminate Thickness.

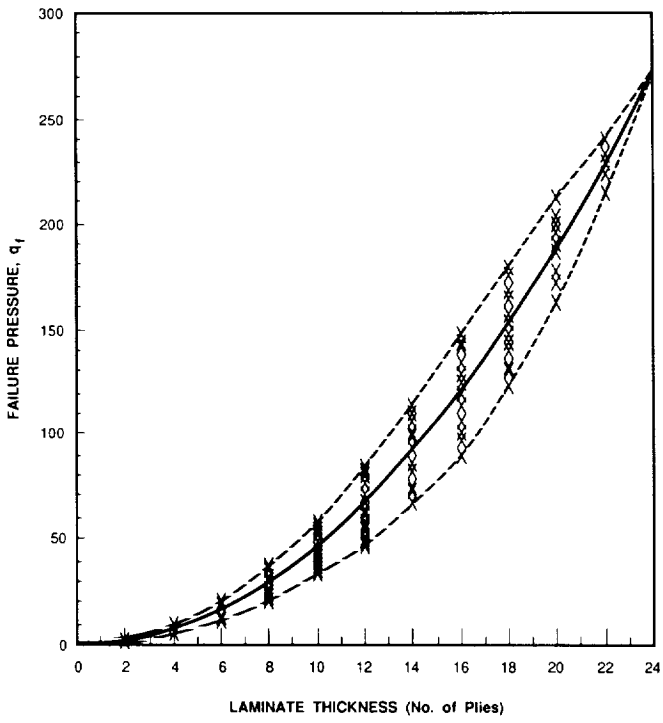

Figure 4. Failure Pressure of a Rectangular Plate as a Function of Plate Thickness.

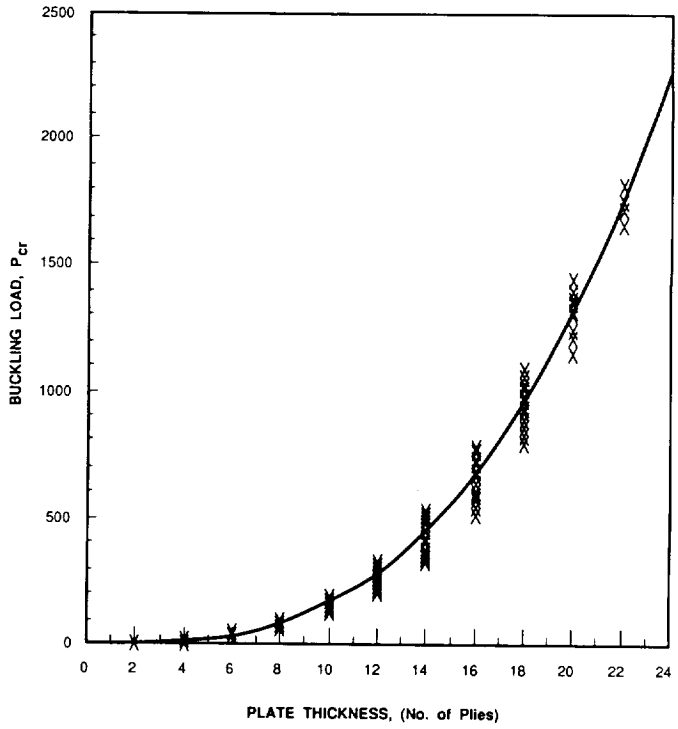

Figure 5. Buckling Load of a Simply Supported Rectangular Plate as a Function of Plate Thickness.

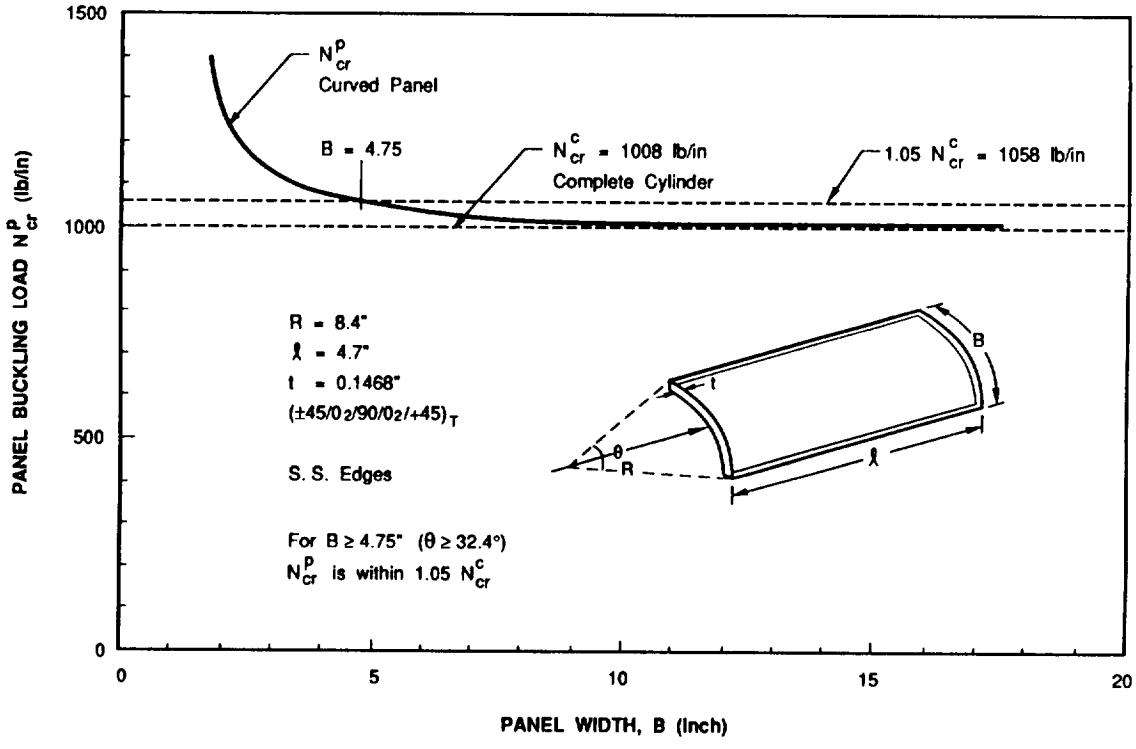

Figure 6. Effect of Panel Width on Buckling Load.

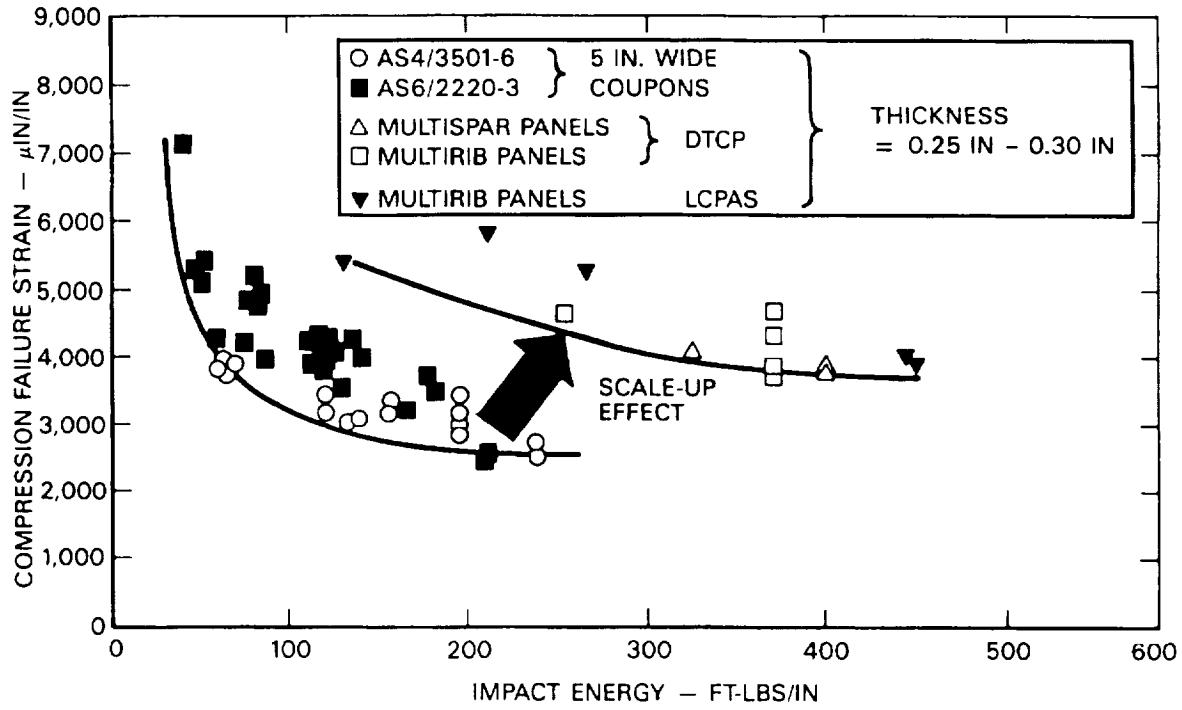

Figure 7. Scale-Up Effects on Post-Impact Compression Strength.

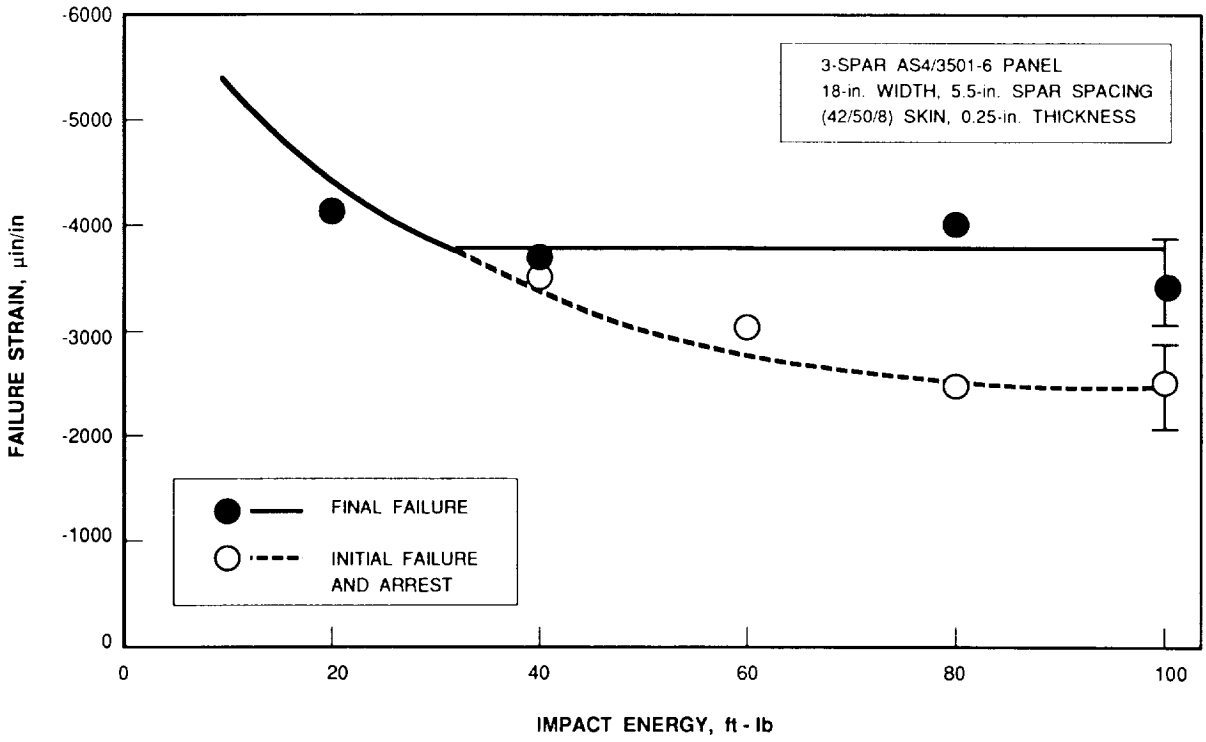

Figure 8. Comparison of Observed and Predicted Strain.

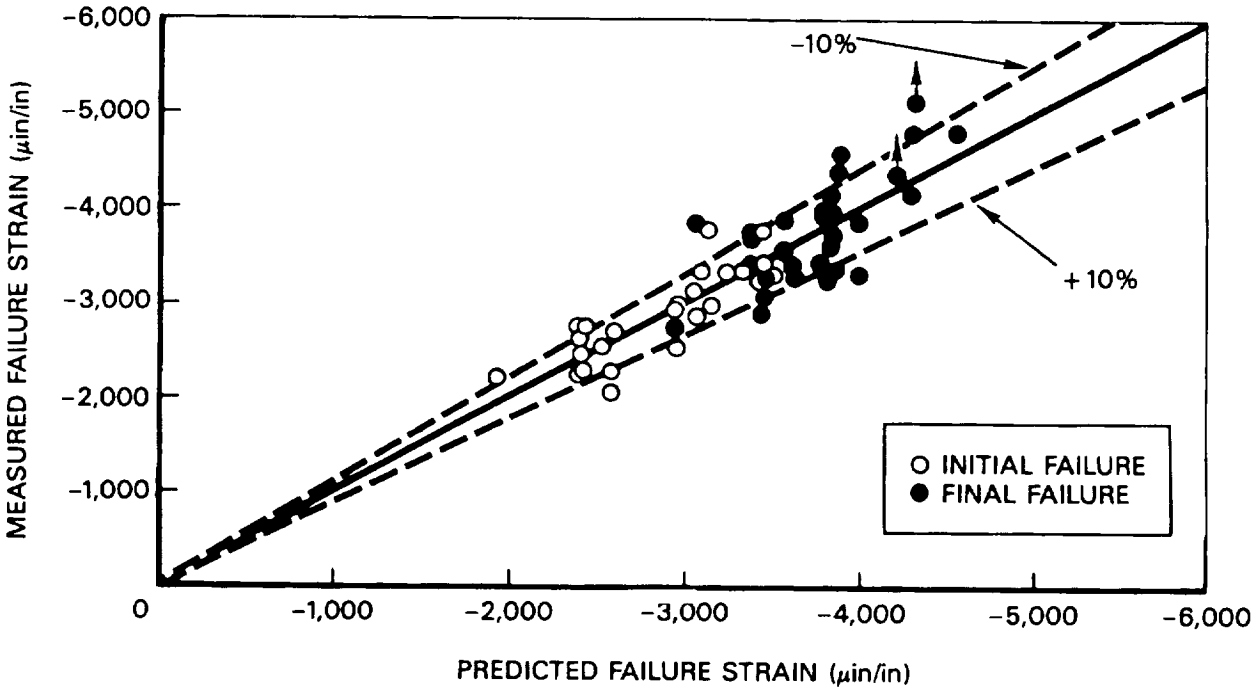

Figure 9. Comparison of Measured and Predicted Post-Impact Compression Strength for Built-Up Structures.

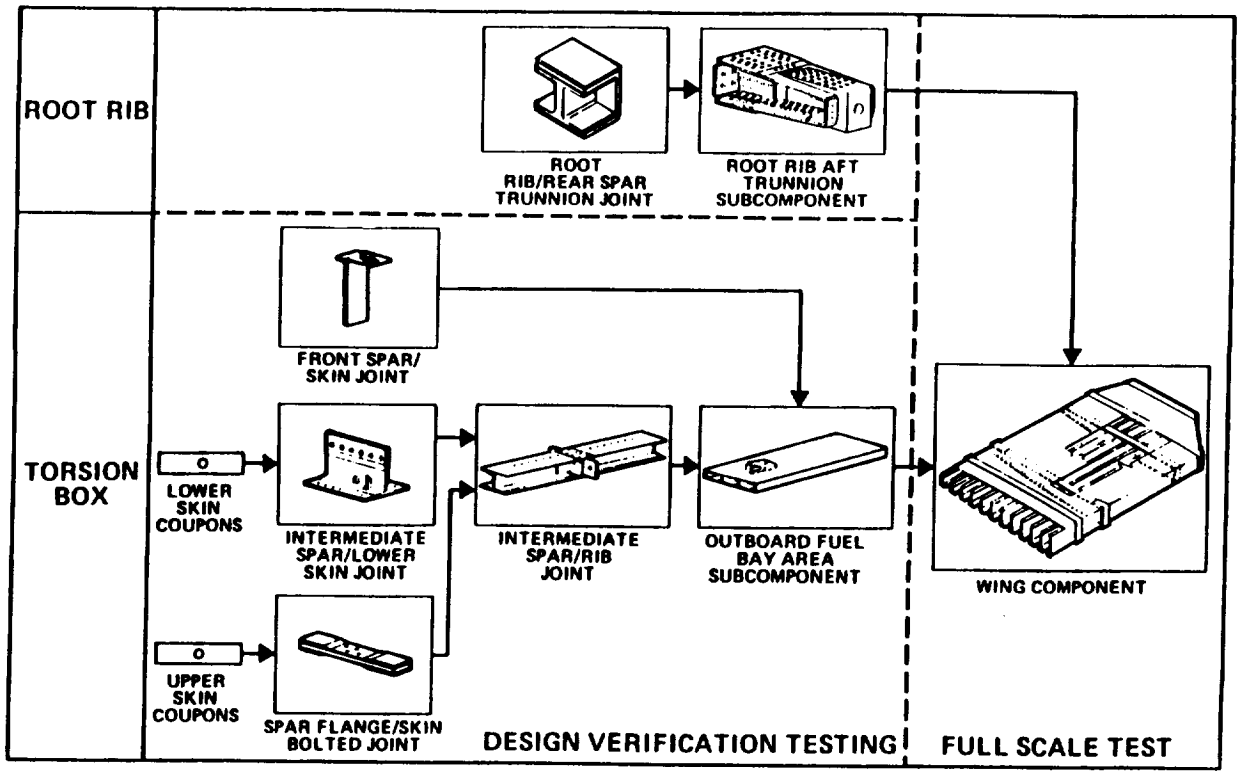

Figure 10. Building Block Approach for the Wing Structure in the Composite Wing/Fuselage Program (Reference 1).